A Singlet Thiophosphoryl Nitrene and Its Interconversion with Thiazyl and Thionitroso Isomers

Hongmin Li,[†] Zhuang Wu,[†] Dingqing Li,[†] Xiaoqing Zeng,*[,†] Helmut Beckers,[‡] and Joseph S. Francisco*[,§]

[†]College of Chemistry, Chemical Engineering and Materials Science, Soochow University, Suzhou 215123, China
[‡]Institut für Chemie und Biochemie, Freie Universität Berlin, D-14195 Berlin, Germany
[§]Department of Chemistry, Purdue University, West Lafayette, Indiana 47907, United States

S *Supporting Information*

ABSTRACT: Thiophosphoryl nitrenes, $R_2P(S)N$, are thiazirine-like intermediates that have been chemically inferred from trapping products in early solution studies. In this work, photolysis of the simplest thiophosphoryl azide, $F_2P(S)N_3$, in solid noble-gas matrices enabled a first-time spectroscopic (IR and UV−vis) identification of the thiophosphoryl nitrene $F_2P(S)N$ in its singlet ground state. Upon visible-light irradiation (≥495 nm), it converts into the thionitroso isomer $F_2P−N{=}S$, which can also be produced in the gas phase from flash vacuum pyrolysis of $F_2P(S)N_3$. Further irradiation of $F_2P−NS$ with 365 nm UV light leads to the reformation of $F_2P(S)N$ and isomerization to the thiazyl species $F_2P−S{\equiv}N$.

Covalent azides are broadly used in chemistry, biology, and materials science.[1] Upon either heat or irradiation, this class of energetic compounds can split off molecular nitrogen and form highly reactive nitrene intermediates.[2] The decomposition of covalent azides, in particular carbonyl,[3] phosphoryl,[4] and sulfonyl azides,[5] has attracted enormous theoretical and experimental interest since the discovery of the Curtius rearrangement from carbonyl azides to isocyanates as early as 1890.[6] Generally, a stepwise decomposition via α-oxonitrenes (RC(O)N, $R_2P(O)N$, and $RS(O)_2N$, respectively) is energetically more favorable than the concerted pathway, and these α-oxonitrenes in their singlet state coexist with an oxazirine-like resonance structure as a result of an intramolecular N−O stabilizing interaction.[3−5] However, because of complex reactions with solvents and the Curtius rearrangement, only very few transient α-oxonitrenes have been detected using ultrafast spectroscopy[3−5] and matrix-isolation techniques.[7] Importantly, the decomposition of α-oxoazides has provided unique access to N,O-containing species bearing novel structural and bonding properties such as N_2CO,[8] OPN,[9] and O_2SN,[10] in which the corresponding α-oxonitrenes were suggested to be involved.

In regard to the heavier sulfur analogues, the structure in α-thionitrenes could be quite different because bonding changes dramatically in going from first-row to second-row elements in the periodic table. For instance, the cyclic sulfur-containing species SiS_2[11] and SNP[12] are isolable, whereas the first-row species SiO_2[13] and OPN[9] prefer only open-chain structures. Thus, singlet α-thionitrenes should be viable species by the formation of a thiazirine ring structure. Indeed, the existence of the singlet thiocarbonyl nitrenes FC(S)N[14] and PhC(S)N[15] was inferred by characteristic IR vibration bands at 1784 and 1160 cm^{-1} in a solid Ar matrix and 1740 cm^{-1} in CH_3CN, respectively. In contrast, knowledge about the structurally related thiophosphoryl nitrene is rather limited, even though its existence has been chemically inferred by Bertrand and co-workers[16] from trapping products during the photolysis of diphenylthiophosphoryl azide.

Herein we report the generation and characterization of the simplest thiophosphoryl nitrene, $F_2P(S)N$ and its photo-induced interconversion with two novel nitrogen−sulfur multiple-bonded isomers, $F_2P−N{=}S$ and $F_2P−S{\equiv}N$. It should be noted that theoretically predicted isomerizations between thiazyl and thionitroso compounds, such as HNS/HSN[17] and FNS/FSN,[17c,18] have not been experimentally observed before.

The generation of difluorothiophosphoryl nitrene, $F_2P(S)N$, was accomplished by ArF laser photolysis (193 nm) of $F_2P(S)N_3$ in solid Ar at 16 K (see the Supporting Information (SI) for details). To distinguish its IR bands (Figure S1 in the SI), subsequent visible-light irradiation (≥495 nm) was applied. The IR difference spectrum showing the corresponding changes is presented as the bottom trace in Figure 1. The two IR bands for the antisymmetric and symmetric F_2P stretches in $F_2P(S)N$ can be clearly identified at 925.5 and 873.2 cm^{-1}, which are lower than those of the precursor (951.8 and 912.9 cm^{-1}, respectively). Another species (**b**) showing the stretching modes of the F_2P(III) moiety with lower frequencies at 845.8 and 817.8 cm^{-1} was partially consumed under this irradiation. As a result, a third species (**c**) having similar vibrations at 842.9 and 825.6 cm^{-1} was produced.

Further irradiation of the matrix with 330 nm UV light leads to complete conversion of **b** to **c** (Figure 1, middle trace). The reverse conversion from **c** to **a** and **b** was observed upon irradiation at 365 nm (Figure 1, top trace). For the nitrene **a**, additional bands at 1189.6 and 631.4 cm^{-1} corresponding to the P−N and P−S stretching vibrations, respectively, can be unambiguously identified. For species **b**, one more band appears at 1175.5 cm^{-1}. Three bands at 1223.5, 649.7, and 626.7 cm^{-1} belonging to **c** can be confirmed, and the first one shows two more site-splitting bands at 1268.7 and 1253.3 cm^{-1},
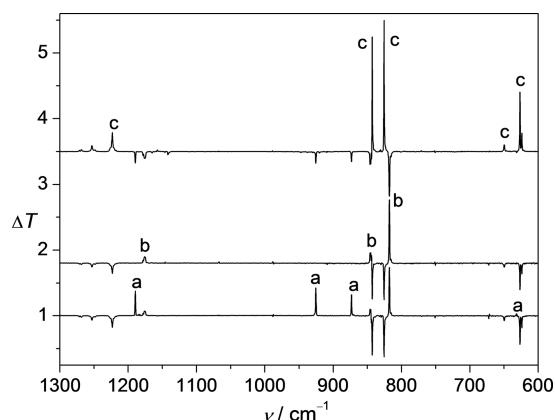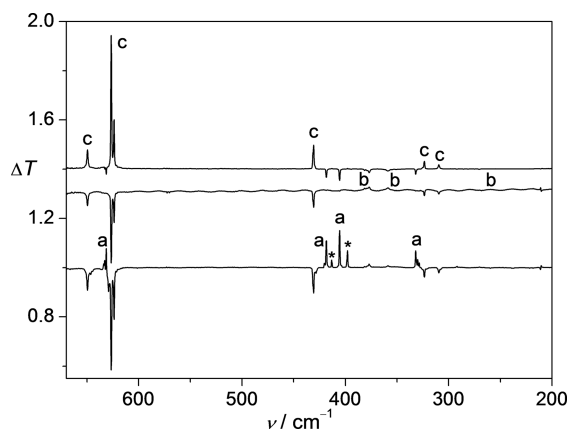
Figure 1. Ar-matrix mid-IR difference spectra (1300−600 cm^{-1}, transmittance T): (bottom trace) conversion of $F_2P(S)N$ (**a**) and F_2PSN (**b**) to F_2PNS (**c**) under irradiation at ≥495 nm (20 min); (middle trace) conversion of F_2PSN (**b**) to F_2PNS (**c**) under irradiation at 330 nm (15 min); (top trace) conversion of F_2PNS (**c**) to $F_2P(S)N$ (**a**) and F_2PSN (**b**) under irradiation at 365 nm (20 min).

probably due to weak interactions with surrounding species in the same solid matrix cages.

Independent photolysis experiments in the far-IR range (700−200 cm^{-1}) were performed using a liquid-helium-cooled bolometer detector. All of the aforementioned photointerconversion reactions were reproduced (Figure 2). Experiments

Figure 2. Ar-matrix far-IR difference spectra (670−200 cm^{-1}, transmittance T): (bottom trace) conversion of $F_2P(S)N$ (**a**) and F_2PSN (**b**) to F_2PNS (**c**) under irradiation at ≥495 nm (20 min); (middle trace) conversion of F_2PSN (**b**) to F_2PNS (**c**) under irradiation at 330 nm (16 min); (top trace) conversion of F_2PNS (**c**) to $F_2P(S)N$ (**a**) and F_2PSN (**b**) under irradiation at 365 nm (20 min). Bands of unknown species are labeled with asterisks.

with ^{15}N-enriched azide ($F_2P(S)^{15}NNN$:$F_2P(S)NN^{15}N$ = 1:1) showed that all of the carriers (**a**−**c**) contain only one nitrogen atom, as evidenced by the well-resolved doublet splitting of the corresponding IR bands (Figures S2 and S3). The observed IR data, including ^{15}N isotopic shifts for species **a**−**c**, are summarized in Table 1. For comparison, the CCSD(T)/aug-cc-pVTZ calculated IR spectra of $F_2P(S)N$ and candidate isomers F_2PSN and F_2PNS are listed.

The band for the PN stretching vibration in $F_2P(S)N$ (**a**) at 1189.6 cm^{-1} exhibits a large ^{15}N isotopic shift of 17.3 cm^{-1}, which is consistent with the prediction of 18.8 cm^{-1}. Such a higher frequency compared with the PN stretching frequencies

for FP=NF (1116.8 cm^{-1})[19] and $F_2P(O)N$ (766.7 cm^{-1})[7c] suggests a P=N double bond in **a**. As a side proof of the assignment, the calculated IR spectrum of triplet $F_2P(S)N$ (Table S1 in the SI) deviates significantly from the experimental observations. An ^{15}N isotopic shift of 8.2 cm^{-1} was found for the symmetric F_2P stretch at 873.2 cm^{-1}, demonstrating its vibrational coupling with the PN stretch. Because of spectral overlap, the expected isotopic shift of 7.6 cm^{-1} for the PS stretch of the naturally abundant ^{34}S sample was not observed.

On the basis of the two pairs of F_2P stretching vibrations at 845.8/817.8 and 842.9/825.6 cm^{-1}, the assignments for F_2PSN (**b**) and F_2PNS (**c**) also become straightforward. In fact, these frequencies are fairly close to the two F_2P stretching vibrations of free-radical F_2P (852.1 and 831.4 cm^{-1}).[20] For species **b**, the highest vibration appears at 1175.5 cm^{-1} with an ^{15}N isotopic shift of 27.0 cm^{-1}. A close inspection of the spectrum reveals an isotopic shift of 10.4 cm^{-1} due to naturally abundant ^{34}S. Similar isotopic shifts ($\Delta\nu(^{15}N)$ = 27.0 cm^{-1}, $\Delta\nu(^{34}S)$ = 6.2 cm^{-1}) were also observed for the highest vibration of **c** at 1223.5 cm^{-1} (Figure 1, top trace). These features are comparable with the IR data for the unperturbed NS radical at 1209.4 cm^{-1} ($\Delta\nu(^{15}N)$ = 28.1 cm^{-1}, $\Delta\nu(^{34}S)$ = 10.8 cm^{-1}).[21]

For F_2PSN (**b**), calculations at the CCSD(T) level of theory overestimate the P−S stretching vibration (calcd, 444 cm^{-1}; exptl, 376.9 cm^{-1}), whereas the P−N stretching vibration is underestimated in F_2PNS (**c**) (calcd, 610 cm^{-1}; exptl, 626.7 cm^{-1}). These differences may suggest weak but complex bonding interactions between the F_2P and NS fragments in these two electron-rich molecules. An additional band at 649.4 cm^{-1} with an ^{15}N isotopic shift of 9.1 cm^{-1} was found for **c**, corresponding to the overtone of ν_6 (323.6 cm^{-1}, $\Delta\nu(^{15}N)$ = 4.5 cm^{-1}). This overtone gains its intensity from the strong P−N stretching mode (ν_4, 626.7 cm^{-1}) through Fermi resonance.

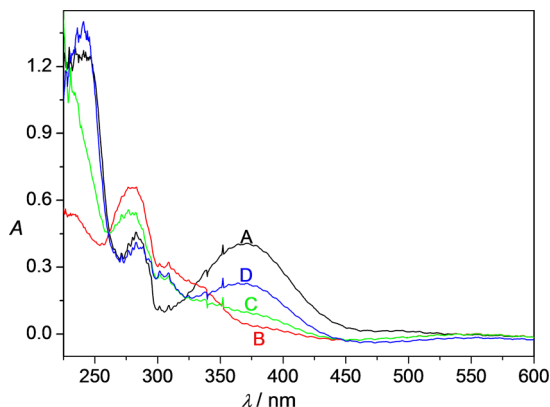Flash vacuum pyrolysis of $F_2P(S)N_3$ in Ar dilution (1:500) at about 800 °C results in complete decomposition, with F_2PNS (**c**) being the main product (Figure S4). The UV−vis spectrum of the pyrolysis products in Ne dilution (1:500) is shown in Figure 3A. Three broad absorption bands at λ_{max} = 370, 285, and 240 nm are observed. They vanish upon irradiation at 365 nm with the occurrence of bands at λ_{max} = 310 and 275 nm (Figure 3B). Thus, the first three bands belong to **c**, and the assignment is assured by the reappearance of these bands upon visible-light irradiation at ≥455 nm (Figure 3D). The absorption at 370 nm is significantly blue-shifted in comparison with the visible absorption bands of $Me_2N−NS$ (587 nm in cyclohexane)[22] and Ar−NS (456 and 483 nm in an Ar matrix).[23] Upon further irradiation at 330 nm (Figure 3C), the band of **c** at 370 nm appears at the expense of the band at 310 nm, and the intensity of the band at 275 nm increases. These changes support the tentative assignment of the bands at 310 and 275 nm to F_2PSN (**b**) and $F_2P(S)N$ (**a**), respectively.

The molecular structures of **a**−**c** (Figure 4) were fully optimized with different density functional theory and ab initio methods (Tables S1−S4). All of the methods conclusively predict that F_2PNS (**c**) is the global minimum on the potential energy surface (Figure S5). The two isomers **a** and **b** are 13.8 and 24.9 kcal mol^{-1} higher in energy, and the nitrene **a** in the triplet state lies 4.7 kcal mol^{-1} above the singlet at the CCSD(T)/aug-cc-pVTZ level. This is consistent with the observation that **c** is the final pyrolysis product of $F_2P(S)N_3$. Even though a stepwise decomposition mechanism for the azide via the intermediacy of **a** (Figure S6) and also a moderate

Table 1. Observed and Calculated IR Frequencies and ^{15}N Isotopic Shifts (in cm^{-1}) for the Fundamental Vibrations of Isomers a−c

F$_2$P(S)N (a)				F$_2$PSN (b)				F$_2$PNS (c)			
calcd[a]	exptl			calcd[a]	exptl			calcd[a]	exptl		
ν_i	ν_i[b]	$\Delta\nu_i$[c]	assignment[d]	ν_i	ν_i[b]	$\Delta\nu_i$[c]	assignment[d]	ν_i	ν_i[b]	$\Delta\nu_i$[c]	assignment[d]
1182	1189.6 (s)	17.3	ν_1, ν(PN)	1141	1175.5 (m)	27.0	ν_1, ν(SN)	1068	1223.5 (m)	27.0	ν_1, ν(SN)
927	925.5 (s)	0	ν_7, ν_{as}(PF$_2$)	835	845.8 (s)	0	ν_2, ν_s(PF$_2$)	859	842.9 (s)	0	ν_2, ν(PF)
868	873.2 (s)	8.2	ν_2, ν_s(PF$_2$)	828	817.8 (s)	0	ν_7, ν_{as}(PF$_2$)	840	825.6 (s)	0	ν_3, ν(PF′)
626	631.4 (w)	0	ν_3, ν(PS)	444	376.9 (w)	0.8	ν_3, δ(PSN)	610	626.7 (s)	6.9	ν_4, ν(PN)
407	418.5 (m)	1.6	ν_4, δ(SPN)	359	358.9 (w)	1.5	ν_4, δ(PF$_2$)	425	430.7 (m)	0	ν_5, δ(F′PN)
393	405.6 (m)	6.9	ν_5, δ(PF$_2$)	214	270.4 (vw)	<0.5	ν_5, ν(PS)	357	323.6 (w)	4.5	ν_6, δ(PF$_2$)
317	331.9 (w)	3.8	ν_8, δ(FPN)	190			ν_8, δ(FPS)	312	309.4 (w)	0.5	ν_7, δ(FPN)

[a]Calculated IR frequencies (in cm^{-1}) for the first seven fundamentals at the CCSD(T)/aug-cc-pVTZ level. A full list of the calculated IR fundamentals and symmetries is given in Table S2. [b]Observed IR band positions with relative intensities in parentheses (s, strong; m, medium-strong; w, weak; vw, very weak). [c]Observed $^{14/15}$N isotopic shifts. [d]Tentative assignments based on calculated vibrational displacement vectors.

Figure 3. Ne-matrix UV−vis spectra of (A) flash vacuum pyrolysis products of F$_2$P(S)N$_3$, (B) after irradiation at 365 nm (40 min), (C) after further irradiation at 330 nm (20 min), and (D) after further irradiation at ≥455 nm (20 min).
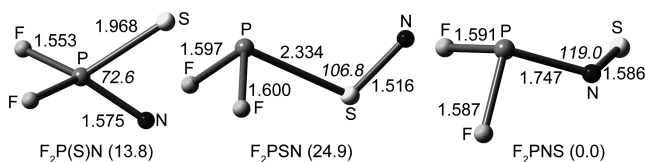

Figure 4. Calculated structures (bond lengths in Å, angles in deg in italics) and relative energies (kcal mol^{-1}, in parentheses) of a−c at the CCSD(T)/aug-cc-pVTZ level.

activation barrier for its rearrangement to **c** (Figure S5) were theoretically predicted, the nitrene **a** can be trapped only in low-temperature matrices from the photolysis of the matrix-isolated azide. The thermal conversion reaction from **c** to **a** or **b** is blocked by large activation barriers (>30 kcal mol^{-1}, CBS-QB3), whereas such barriers can be surmounted by using irradiations at different wavelengths.

The θ(SPN) angle in F$_2$P(S)N is 72.6°, which is much narrower than that in the triplet state (112.8°). The S−N bond length (2.121 Å) is longer than that in cyclic PSN (1.934 Å).[12] Therefore, its structure can be illustrated by nitrene and thiazirine-like forms (Scheme 1), with the latter being more favorable, as indicated by the S−N bonding interactions in the highest occupied molecular orbitals (Figure S7) and the Wiberg bond index of 0.9 with significant negative charge on the nitrogen atom (−1.0e) given by natural bond orbital analysis (Figure S8). The thionitroso compound R−NS can also be

Scheme 1. Lewis Resonance Structures of a−c
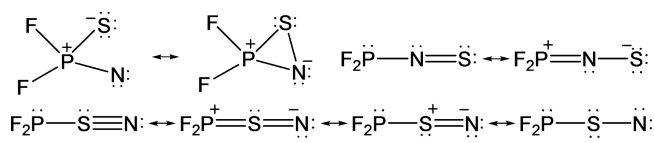
stabilized by two resonance structures (Scheme 1). The preference for a formal N=S double bond[24] in F$_2$P−NS is evidenced by the calculated bond length of 1.586 Å and the accompanying IR frequency of 1175.5 cm^{-1}. However, the preference for a formal N−S single bond was found in the thionitrosoamine Me$_2$N−NS, as proved by a bond length of 1.635(2) Å in the pentacarbonylchromium complex via the sulfur atom.[25] The bonding situation in F$_2$PSN is more complicated by several possible canonical forms (Scheme 1). Previous studies concluded that decreasing the electronegativity of R in thiazyl compounds R−SN stabilizes the polar or nitrene-type structures and vice versa.[26] Thus, a formal sulfur triple bond was found in F−SN (r_{SN} = 1.448 Å, ν_{SN} = 1361 cm^{-1}),[26] and a nitrene intermediate structure was proposed for Ar−SN on the basis of its reactivity.[27] The long S−N bond in F$_2$P−SN (r_{SN} = 1.516 Å, ν_{SN} = 1223.5 cm^{-1}) indicates a favorable polar structure with a formal double bond.

In summary, the three novel isomeric species F$_2$P(S)N, F$_2$P-SN, and F$_2$P-NS were generated through stepwise photolysis of F$_2$P(S)N$_3$. Their structures, energies, and bonding properties have been analyzed on the basis of spectroscopic data and quantum-chemical calculations. The nitrene F$_2$P(S)N has singlet ground state that is stabilized by the formation of a rare thiazirine-like ring structure containing $\sigma^4\lambda^5$-phosphorus. The other two isomers F$_2$P−SN and F$_2$P−NS, bearing sulfur−nitrogen multiple bonds, represent the first couple of experimentally established thiazyl and thionitroso compounds that can be reversibly interconverted. In particular, the facile production of F$_2$P−NS in the gas phase will stimulate future studies of the structure and reactivity of unstable thionitroso compounds.

■ ASSOCIATED CONTENT

ⓢ Supporting Information

The Supporting Information is available free of charge on the ACS Publications website at DOI: 10.1021/jacs.5b07302.

Experimental details, calculation methods, matrix IR spectra, and calculated results for F$_2$PNS isomers (PDF)

■ AUTHOR INFORMATION

Corresponding Authors

*xqzeng@suda.edu.cn
*francisc@purdue.edu

Notes

The authors declare no competing financial interest.

■ REFERENCES

(1) *Organic Azides: Syntheses and Applications*; Bräse, S., Banert, K., Eds.; John Wiley & Sons: Chichester, U.K., 2010.

(2) (a) *Nitrenes and Nitrenium Ions*; Falvey, D. E., Gudmundsdottir, A. D., Eds.; Wiley Series on Reactive Intermediates in Chemistry and Biology, Vol. 6; John Wiley & Sons: Hoboken, NJ, 2013. (b) Gritsan, N. P.; Platz, M. S.; Borden, W. T. The Study of Nitrenes by Theoretical Methods. In *Computational Methods in Photochemistry*; Kutateladze, A., Ed.; Molecular and Supramolecular Photochemistry, Vol. 13; CRC Press: Boca Raton, FL, 2005. (c) *Reactive Intermediate Chemistry*; Moss, R. A., Platz, M. S., Jones, M. J., Jr., Eds.; John Wiley & Sons: Hoboken, NJ, 2004.

(3) For recent examples, see: (a) Kubicki, J.; Zhang, Y.; Vyas, S.; Burdzinski, G.; Luk, H. L.; Wang, J.; Xue, J.; Peng, H.-L.; Pritchina, E. A.; Sliwa, M.; Buntinx, G.; Gritsan, N. P.; Hadad, C. M.; Platz, M. S. *J. Am. Chem. Soc.* **2011**, *133*, 9751. (b) Kubicki, J.; Zhang, Y.; Wang, J.; Luk, H. L.; Peng, H.-L.; Vyas, S.; Platz, M. S. *J. Am. Chem. Soc.* **2009**, *131*, 4212. (c) Sherman, M. P.; Jenks, W. S. *J. Org. Chem.* **2014**, *79*, 8977. (d) Desikan, V.; Liu, Y.; Toscano, J. P.; Jenks, W. S. *J. Org. Chem.* **2008**, *73*, 4398. (e) Murthy, R. S.; Muthukrishnan, S.; Rajam, S.; Mandel, S. M.; Ault, B. S.; Gudmundsdottir, A. D. *J. Photochem. Photobiol., A* **2009**, *201*, 157. (f) Wentrup, C.; Bornemann, H. *Eur. J. Org. Chem.* **2005**, *2005*, 4521.

(4) Vyas, S.; Muthukrishnan, S.; Kubicki, J.; McCulla, R. D.; Burdzinski, G.; Sliwa, M.; Platz, M. S.; Hadad, C. M. *J. Am. Chem. Soc.* **2010**, *132*, 16796 and references therein..

(5) (a) Kubicki, J.; Luk, H. L.; Zhang, Y.; Vyas, S.; Peng, H.-L.; Hadad, C. M.; Platz, M. S. *J. Am. Chem. Soc.* **2012**, *134*, 7036. (b) Kubicki, J.; Zhang, Y.; Xue, J.; Luk, H. L.; Platz, M. S. *Phys. Chem. Chem. Phys.* **2012**, *14*, 10377 and references therein..

(6) Curtius, T. *Ber. Dtsch. Chem. Ges.* **1890**, *23*, 3023.

(7) (a) Zeng, X. Q.; Beckers, H.; Willner, H.; Grote, D.; Sander, W. *Chem. - Eur. J.* **2011**, *17*, 3977. (b) Zeng, X. Q.; Beckers, H.; Willner, H. *J. Am. Chem. Soc.* **2013**, *135*, 2096. (c) Zeng, X. Q.; Beckers, H.; Willner, H.; Neuhaus, P.; Grote, D.; Sander, W. *Chem. - Eur. J.* **2009**, *15*, 13466.

(8) Zeng, X. Q.; Beckers, H.; Willner, H.; Stanton, J. F. *Angew. Chem., Int. Ed.* **2011**, *50*, 1720.

(9) Zeng, X. Q.; Beckers, H.; Willner, H. *J. Am. Chem. Soc.* **2011**, *133*, 20696.

(10) Zeng, X. Q.; Beckers, H.; Willner, H. *Angew. Chem., Int. Ed.* **2013**, *52*, 7981.

(11) Mück, L. A.; Lattanzi, V.; Thorwirth, S.; McCarthy, M. C.; Gauss, J. *Angew. Chem., Int. Ed.* **2012**, *51*, 3695.

(12) Zeng, X. Q.; Beckers, H.; Willner, H.; Francisco, J. S. *Angew. Chem., Int. Ed.* **2012**, *51*, 3334.

(13) Schnöckel, H. *Angew. Chem., Int. Ed. Engl.* **1978**, *17*, 616.

(14) Pasinszki, T.; Bazsó, G.; Krebsz, M.; Tarczay, G. *Phys. Chem. Chem. Phys.* **2009**, *11*, 9458.

(15) Liu, Y.; Evans, A. S.; Toscano, J. P. *Phys. Chem. Chem. Phys.* **2012**, *14*, 10438.

(16) (a) Baceiredo, A.; Bertrand, G.; Majoral, J.-P.; Anba, F. E.; Manuel, G. *J. Am. Chem. Soc.* **1985**, *107*, 3945. (b) Bertrand, G.; Majoral, J.-P.; Baceiredo, A. *Acc. Chem. Res.* **1986**, *19*, 17.

(17) (a) Ben Yaghlane, S.; Jaidane, N.-E.; Cotton, C. E.; Francisco, J. S.; Al Mogren, M. M.; Linguerri, R.; Hochlaf, M. *J. Chem. Phys.* **2014**, *140*, 244309. (b) Sato, K.; Takayanagi, T. *Chem. Phys.* **2015**, *450−451*, 74. (c) Takeshita, T. Y.; Dunning, T. H., Jr. *J. Phys. Chem. A* **2015**, *119*, 1446. (d) Denis, P. A.; Ventura, O. N.; Mai, H. T.; Nguyen, M. T. *J. Phys. Chem. A* **2004**, *108*, 5073.

(18) Schaad, L. J.; Hess, B. A., Jr.; Čársky, P.; Zahradník, R. *Inorg. Chem.* **1984**, *23*, 2428.

(19) Zeng, X. Q.; Beckers, H.; Willner, H. *Angew. Chem., Int. Ed.* **2009**, *48*, 4828.

(20) Current, J. H.; Burdett, J. K.; Hodges, L.; Dunning, V. *J. Phys. Chem.* **1970**, *74*, 4053.

(21) Hassanzadeh, P.; Andrews, L. *J. Am. Chem. Soc.* **1992**, *114*, 83.

(22) Middleton, W. J. *J. Am. Chem. Soc.* **1966**, *88*, 3842.

(23) Takahashi, M.; Okazaki, R.; Inamoto, N.; Sugawara, T.; Iwamura, H. *J. Am. Chem. Soc.* **1992**, *114*, 1830.

(24) Pyykkö, P.; Riedel, S.; Patzschke, M. *Chem. - Eur. J.* **2005**, *11*, 3511.

(25) Roesky, H. W.; Emmert, R.; Clegg, W.; Isenberg, W.; Sheldrick, G. M. *Angew. Chem., Int. Ed. Engl.* **1981**, *20*, 591.

(26) Glemser, O.; Mews, R. *Angew. Chem., Int. Ed. Engl.* **1980**, *19*, 883.

(27) Atkinson, R. S.; Judkins, B. D. *J. Chem. Soc., Chem. Commun.* **1979**, 833.